Optical Characterization of Ferric-Doped ZnO Thin Film Deposited By Chemical Bath Deposition Method

Mohammad Shahjahan[1*], Aktarunnahar Eseta[2], Mohammad Asadul Haque[3]

[1, 2, 3]Department of Physics, University of Chittagong, Chittagong-4331, Bangladesh.
Email: [1]shahjahan@cu.ac.bd, [2]eshita.physics49@gmail.com, [3]asad2310@gmail.com

Abstract – *Fe-doped ZnO holds numerous potential uses in devices such as UV light emitters, piezoelectric transducers, transparent electronics in solar cells, and bright windows as an II-VI semiconductor material. This study looked into the band gap, surface characteristics, optical transmittance, and absorbance of ZnO thin films with Fe doping in different pH conditions such as 8, 9, and 10. The films were prepared using the chemical bath deposition (CBD) method at 350 °C on a glass substrate. The samples were characterized using UV-visible spectroscopy and scanning electron microscopy (SEM). The SEM images of the undoped samples exhibited a lack of cracks, but the doped samples displayed visible cracks due to the presence of Fe in the films. ZnO thin-film surface shape is altered by pH and Fe doping variations. There is a tendency for the films' visual transmission to decrease when the pH rises. The absorbance for all samples increases in the UV and declines in the visible. Fe doping causes the optical band gap Eg to drop. The band gap of both doped and undoped samples reduces when pH rises.*

Keywords: *Zinc oxide; metal oxide; chemical bath; optical properties; transmittance.*

1. Introduction

The field of thin solid films has recently evolved in response to the demand for enhanced electrical and optical devices in industrial and military sectors [1-2]. This field of study has moreover presented intriguing prospects for fundamental investigation. Thin film technology is a significant specialized field that focuses on studying the properties of various metals [3], semiconductors [4], and insulators when they are in the form of thin films [5]. The characteristics of thin films exhibit notable distinctions when compared to their corresponding bulk properties [6]. Thin film research has garnered significant relevance due to its wide-ranging applications in the fields of electronics [7], optics [8], space science [9], and various industries.

Semiconductor thin films hold significant importance in the field of materials science owing to their exceptional electrical and optical properties, which find utility in a wide range of optoelectronic devices [10]. The systematic investigation of semiconducting films has been ongoing for decades. In the early stages of research, there was a focus on investigating elemental semiconducting films such as silicon (Si) and germanium (Ge). In contemporary times, researchers have been notably interested in emerging semiconductors such as oxide and sulphide. Extensive investigation and experimentation in the field of thin films have yielded the finding that several categories of materials exhibit notable suitability for specific applications.

Extensive research has been conducted on ZnO, a semiconductor material characterized by its broad energy band gap. The material exhibits a notable bonding energy of 60 MeV, leading to reduced carrier entrapment and enhanced luminescence efficiency [11]. The recent focus on ZnO diluted with transition metals has been driven by the growing interest in semiconductor spin-electronics that aims to utilize the spin degree of freedom of charge carriers in semiconductors [12-13]. There is a prevailing anticipation throughout the scientific community regarding the potential to extract innovative functions for electronics and photonics through the injection, transmission, and detection of carrier spin at ambient temperature. Various methods have been employed for the synthesis of ZnO films, including pulsed-laser deposition [14], molecular beam epitaxy [15], chemical bath deposition [16], chemical vapour deposition [17], physical vapour deposition [18] evaporation [19], casting [20], and sputtering [21].

The chemical bath deposition technique is a straightforward and cost-effective processing approach, particularly in terms of equipment expenses. This method provides a highly accessible approach to preparing films of varying compositions. The chemical bath deposition (CBD) technique for the deposition of metal oxides has garnered significant attention owing to its straightforward methodology and the comparatively low temperature required for the operation. Numerous researchers have employed the CBD technique to produce various metal oxides, including ZnO, CuO, CdO, TiO_2, NiO, and others [22].

Previous studies on ZnO have indicated that the enhancement of its optical and electrical properties for use in diverse optoelectronic devices necessitates the inclusion of appropriate impurities. [23] The study of doping using group-III [24] or Group-V [25] elements were conducted by scientists in the 1980s. The study by [26] presents an analysis of the characterization of high-quality ZnO thin films, highlighting the potential for quantum-size particle generation. The number of study fields in ZnO has significantly increased during the past two decades.

Suwanboon et al. [27] conducted a study on the impact of aluminum (Al) and manganese (Mn) dopants on the structural and optical properties of (ZnO) thin films prepared through the sol-gel route. The findings revealed a decrease in the average grain size, with Al ions playing a significant role in enhancing the alignment along the c-axis. Conversely, the presence of Mn ions hindered growth along the c-axis. In their study, Ilican et al. [28] employed the sol-gel spin coating technique to deposit a ZnO thin film onto glass substrates. By varying the chuck rotation rates, the researchers investigated the optical absorption data and observed a direct band gap energy transition. Based on their findings, they suggested that the resulting ZnO thin films hold potential for application as photovoltaic materials. B.P. Kafle et al. [29] conducted a study on the structural, morphological, and optical characteristics of transparent thin films of Fe-doped ZnO using spin coating techniques. Their research findings were the transmittance of the doped film experienced a reduction of approximately 10% and the band gap, for both doped and undoped samples, exhibited no dependence on the concentration of the dopant.

In a study conducted by Rosari Saleh et al. [30], the researchers investigated the impact of varying Fe doping concentrations on the structural, magnetic, and optical characteristics of nanocrystalline ZnO particles using the sol-gel method and were deposited on both Si and glass substrates. It has been observed that the grain sizes of ZnO tend to shrink as the concentration of Fe-doping increases. The inclusion of Fe did not result in a substantial alteration of transmittance within the visible range and band-gaps of ZnO thin films exhibited a gradual increase as the concentration of Fe-doping improved.

In this study, zinc oxide thin films were fabricated using the chemical bath approach, both with and without the incorporation of Fe doping. Considering the Fe doping, it is expected that the optical characteristics will be enhanced. Based on existing understanding, this represents a singular observation of ZnO thin film. This article presents an analysis of the film deposition process, surface morphology, and optical properties, providing valuable insights for many applications like transparent electrode displays and metal-insulator-semiconductor diodes [31].

2. Materials and Methods

Zinc oxide thin films were fabricated on glass substrates using the CBD technique. The trials were initially conducted at ambient temperature without any temperature regulation. The deposition process was initiated by combining 0.3 M solution of zinc nitrate ($Zn(NO_3)_2$), 35% ammonia solution (NH_3), and ferric oxide (Fe_2O_3). To commence the experiment, solutions of zinc nitrate, ammonia were made and subsequently combined using a stirrer, with the mixing process lasting for a duration of 30 minutes. The beaker exhibits a distinct solution. Subsequently, solutions of ammonia were gradually introduced in order to ascertain the buffer condition of the solution. The solution is divided equally into two separate beakers, with each beaker containing an equal volume of the solution. The pH of the both solution is regulated and maintained within the range of 8 to 10 with the addition of ammonia.

The addition of ferric oxide in one beaker solution was performed gradually, accompanied by vigorous stirring for a duration of up to 30 minutes, until a stable solution was achieved and afterwards half both undoped and doped solutions is subjected to a temperature of 85 °C within a microwave oven for 30 minutes. The substrates were immersed in the both hot and cold solution for a duration of 30 s alternatively. The process is repeated 30 times until the film is formed on the substrate. Following the deposition process, the created thin films underwent a thorough rinsing with an adequate amount of distilled water, after which they were left exposed to ambient air for the purpose of drying. Prior to the deposition process, the glass slides underwent thorough cleansing utilizing an ultrasonic cleaner and purified water. The vertical

orientation of the glass slides was observed within the reaction chamber. Subsequently, the ZnO samples that had been deposited were subjected to annealing at a temperature of 350 °C within an argon atmosphere, with the purpose of examining the impact of Fe doping on the films properties. Subsequently, the equipment conducted optical and morphological measurements, respectively.

3. Result and Discussion

3.1 Morphological characterization

The microstructure images of the ZnO thin films were studied using scanning electron microscopy (SEM) in order to obtain microscopic details on the surface structure and roughness. Photographs were captured at varying levels of magnification, as depicted in Fig. 1, for each of the samples. All captured images showed prepared samples have the homogeneity all over the region with agglomerated components in its surface. The visual evidence indicated that the substrate exhibited no significant cracks or pinholes, but

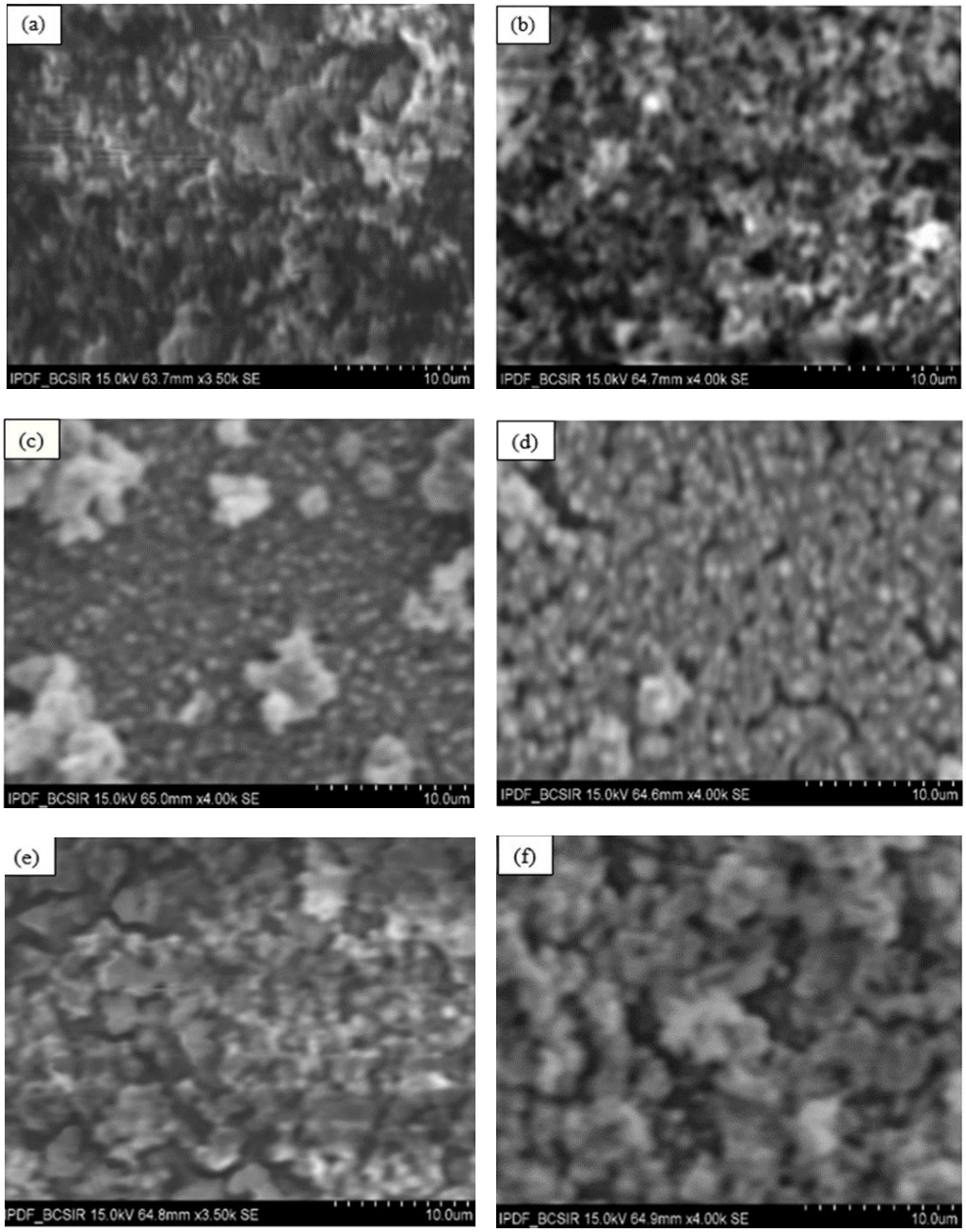

Figure 1. SEM micrograph of ZnO thin film annealed at 350 ^{0}C (a) undoped and (b) doped at pH 8, (c) undoped and (d) doped at pH 9, (e) undoped and (f) doped at pH 10.

changes its size with increasing tendency with pH at undoped condition for all undoped samples (Fig. 1a, Fig 1c, and Fig 1e). Also, at doping states it seems that the images of doped samples (Fig. 1b, Fig. 1d, and Fig. 1e) have significant crack holes and fracture with size increasing with increasing pH. This is suggesting that coating has significant effect on the deposited material. It is apparent that incorporation of Fe dopants in ZnO thin film changed the grain size and grain distribution which crakes the surface. The size of grain has increased after doping. The influence of pH has a positive correlation with a marginal increase in grain size also. However, it does not yield any improvement in surface roughness.

3.2 Optical characterization of ZnO thin films

The optical properties of the film deposited on glass substrate were determined from the absorbance and transmittance measurement in the range of 220 -1400 nm.

3.2.1 Absorbance properties

The figures presented in Fig. 2 illustrate the absorbance spectra of the deposited films within the wavelength range of the 220 nm region. Figure 2 illustrate the relationship between absorbance (expressed in arbitrary units) and wavelength λ (measured in nanometers) for undoped and doped ZnO thin films with pH values of 8, 9, and 10, respectively. Based on the observed data, it can be observed that the absorbance of the ZnO thin film exhibits a rise beyond the wavelength of around 400 nm subsequent to the doping of the film. It was also observed that the absorbance reaches its maximum value at a wavelength of 288 nm for undoped thin films and 285 nm for doped thin films deposited at a pH of 8. Similarly, at a pH of 9, the absorbance is highest at a wavelength of 302 nm for undoped thin films and 288 nm for doped thin films. Lastly, at a pH of 10, the absorbance peaks at a wavelength of 300 nm for undoped thin films and 293 nm for doped thin films. The presence of a distinct absorption edge in the obtained data provides evidence for the favorable optical band edge characteristics shown by the ZnO thin film. The primary absorption phenomenon, which entails the transition of an electron from the valence band to the conduction band, can be employed for the determination of the characteristics and magnitude of the optical band gap.

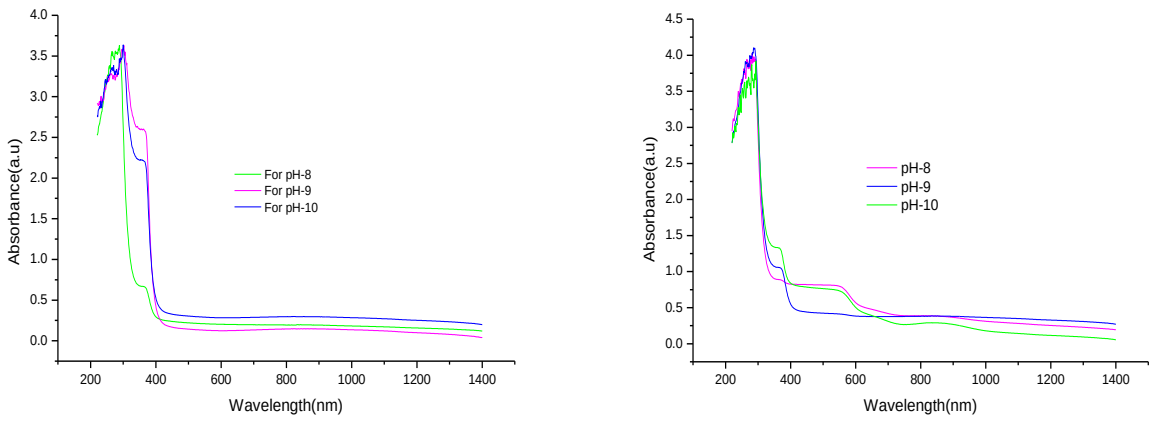

a) b)

Figure 2. Variation of absorbance (a.u.) with wavelength λ (nm) for (a) undoped and (b) doped ZnO thin film deposited at different pH.

3.2.2 Transmittance properties

Figure 3 depicts the transmittance spectra of the ZnO thin film at different pH values (8, 9, and 10) for both doped and undoped films. The data clearly indicates that the optical transmittance exhibits a rise within the visible area and a reduction within the ultraviolet region across all samples. The range of wavelengths used to measure transmittance is 220 -1400 nm. However, within the visible range, there is a progressive decline in the transmittance spectra of the samples as the pH increases, as depicted in Fig. 3. From both figures (Fig. 3a and 3b), it was seen that the transmittance of the film reduced following the process of doping.

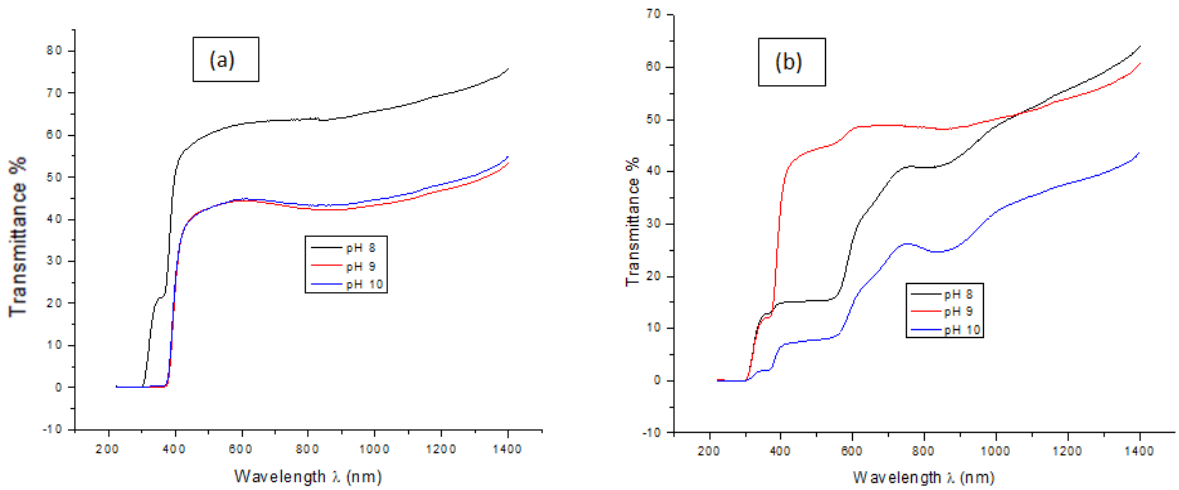

Figure 3. Variation of transmittance (%) with wavelength λ (nm) for (a) undoped and (b) ZnO thin films annealed at 350 ^{0}C.

3.3 Band gap measurement

The determination of the optical band gap (E_g) was carried out by analyzing the plots of $(\alpha h\nu)^2$ to photon energy ($h\nu$) for the respective wavelength (λ) of both undoped and doped ZnO thin films. The symbol α represents the coefficient of absorption. The determination of α can be conducted by the utilization of either transmittance or absorbance measurement techniques. In this research, α was measured using transmittance [32] as the primary method of analysis. The absorption coefficient has been determined from the optical data by the analysis of the transmission spectra, employing the appropriate mathematical relationship [32].

$$\alpha = -\frac{lnT}{t} \tag{1}$$

Where, T is the normalized transmittance and t is the thickness of the film estimated by the following formula [32].

$$t = \frac{(w_2 - w_1)}{A\rho} \times 10^4\ \mu m \tag{2}$$

Where w_1 and w_2 are the weights in (g) of the substrate before and after film deposition, A is the area of film deposition in cm^2, and ρ is the theoretical density of ZnO (5.6 g/cm^3).

Extrapolating the straight line portion of the curve in the energy axis gives the values of band gap energy (Eg) as shown in Fig. 4. The band gap obtained from Fig. 4 is given in Table 1. It is evident that the band gap also decreases with increasing pH and increases after Fe doping. The optical band gap of the samples was higher than the 3.37 eV optical band gap of normal ZnO. Burstein-Moss effect [33] is responsible for this energy shift in the band gap [34].

3.4 Discussion

The deposition of undoped and ferric-doped ZnO thin films onto a glass substrate with 350 °C annealing temperature was carried out utilizing the chemical bath deposition method, with the pH value being varied. The investigation is to check the impact of Fe doping on the thickness, morphological characteristics, and optical properties of the produced samples. Based on the optical analysis conducted on the deposited films, the subsequent results can be inferred. The bath temperature was around 350 °C, which is comparatively lower than the other related research [30].

Table 1: Band gap values of the ZnO thin films deposited at different pH.

pH value	Undoped film (eV)	Doped film (eV)
8	3.9	4.0
9	3.4	3.9
10	3.7	3.8

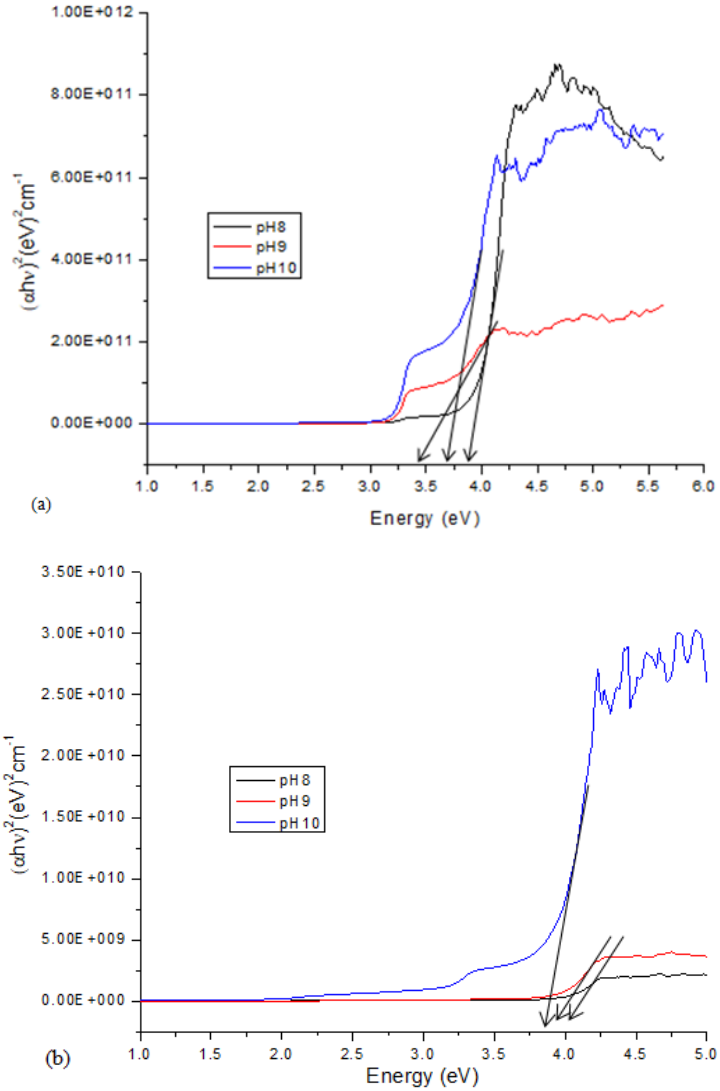

Figure 4. Variation of $(\alpha h\nu)^2$ with photon energy(hν) for (a) undoped and (b) ZnO with different pH.

The morphological and optical characteristics of the prepared sample were dramatically altered by the ferric doping, which served as a modifying agent. The surface morphology of the prepared ZnO thin films is observed to be altered by the changing of pH and ferric doping, as evidenced by SEM micrographs represented in Fig. 1b, Fig. 1d, and Fig. 1f. The images indicated that the films have the expected morphology and homogeneity but grain agglomeration is observed in lower pH deposition as in Fig. 1a. The particle size has increasing tendency in undoped films. The Fe concentration is cracked on the surfaces of the films, keeping the size-increasing tendency unchanged, as represented in Fig. 1b, Fig. 1d, and Fig. 1f.

The optical transmittance spectra of the samples were analyzed, revealing that the visual transmission of the films tends to decrease as the pH increases. The absorbance spectra reveal a consistent pattern across all samples, wherein the absorbance values exhibit a drop within the visible range and an increase within the UV region. The decrease in the optical band gap Eg can be attributed to the exchange interaction that occurs between the localized d shell electrons of the magnetic ions and the delocalized band states. The band gap of both undoped and doped samples exhibits a reduction in response to changes in pH.

The distinctive characteristic of ZnO films, especially the wide bandgap property presented in Table 1 at Fe-doped conditions, can be effectively utilized for the production of transparent electrodes [31] in flat panel displays and metal-insulator-semiconductor diodes. These applications have the potential to substitute p-n junctions by harnessing the electroluminescence of ZnO, thereby circumventing the challenges associated with achieving consistent and dependable p-type ZnO.

4. Conclusion

This study explains the optical characterization of ferric-doped ZnO thin film deposited by the CBD method. The results showed that CBD could be used to create ferric-doped ZnO thin films at a comparatively low bath temperature of about 350 ^{0}C. ZnO thin-film surface shape is altered by pH and Fe doping variations. There is a tendency for the films' visual transmission to decrease when the pH rises. The absorbance for all samples increases in the UV and declines in the visible. Fe doping causes the optical band gap Eg to drop. The band gap of both doped and undoped samples reduces when pH rises. ZnO films' special quality can be utilized to create transparent electrodes that are utilized for a variety of purposes, which could play a major role in solving the present difficulty of available ZnO.

Acknowledgement

We would like to express our sincere gratitude to the Department of Physics at the University of Chittagong, as well as the university administration, for their generous, support, and authorization, which have enabled us to conduct this research project. Acknowledgements are also owed to the entire staff of the Industrial Physics Division of BCSIR Laboratories in Dhaka. We would like to express our gratitude to the Director of BCSIR Laboratories Dhaka for providing us with access to the necessary research facilities.

References

[1] E. Acosta, "Thin Films/Properties and Applications," in *Thin Films*, IntechOpen, 2021. doi: 10.5772/intechopen.95527.

[2] M. W. Cole, W. D. Nothwang, and G. P. Carman, "Advanced Active Thin Films for the Next Generation of Meso-Micro Scale Army Applications," *Ferroelectrics*, vol. 342, no. 1, pp. v–ix, Oct. 2006, doi: 10.1080/00150190600946047.

[3] L. Britnell *et al.*, "Strong Light-Matter Interactions in Heterostructures of Atomically Thin Films," *Science (80-.).*, vol. 340, no. 6138, pp. 1311–1314, Jun. 2013, doi: 10.1126/science.1235547.

[4] Y. Diao, L. Shaw, Z. Bao, and S. C. B. Mannsfeld, "Morphology control strategies for solution-processed organic semiconductor thin films," *Energy Environ. Sci.*, vol. 7, no. 7, pp. 2145–2159, 2014, doi: 10.1039/C4EE00688G.

[5] A. Richardella, A. Kandala, J. S. Lee, and N. Samarth, "Characterizing the structure of topological insulator thin films," *APL Mater.*, vol. 3, no. 8, Aug. 2015, doi: 10.1063/1.4926455.

[6] L. Punga *et al.*, "Studies of the Structure and Optical Properties of BaSrMgWO6 Thin Films Deposited by a Spin-Coating Method," *Nanomaterials*, vol. 12, no. 16, p. 2756, Aug. 2022, doi: 10.3390/nano12162756.

[7] G. Eda and M. Chhowalla, "Graphene-based Composite Thin Films for Electronics," *Nano Lett.*, vol. 9, no. 2, pp. 814–818, Feb. 2009, doi: 10.1021/nl8035367.

[8] D. E. Aspnes, "Optical properties of thin films," *Thin Solid Films*, vol. 89, no. 3, pp. 249–262, Mar. 1982, doi: 10.1016/0040-6090(82)90590-9.

[9] C. M. Lew, R. Cai, and Y. Yan, "Zeolite Thin Films: From Computer Chips to Space Stations," *Acc. Chem. Res.*, vol. 43, no. 2, pp. 210–219, Feb. 2010, doi: 10.1021/ar900146w.

[10] A. Raidou *et al.*, "Characterization of ZnO Thin Films Grown by SILAR Method," *OALib*, vol. 01, no. 03, pp. 1–9, 2014, doi: 10.4236/oalib.1100588.

[11] J. Gutowski, N. Presser, and I. Broser, "Acceptor-exciton complexes in ZnO: A comprehensive analysis of their electronic states by high-resolution magnetooptics and excitation spectroscopy," *Phys. Rev. B*, vol. 38, no. 14, pp. 9746–9758, Nov. 1988, doi: 10.1103/PhysRevB.38.9746.

[12] Y. Z. Peng, T. Liew, W. D. Song, C. W. An, K. L. Teo, and T. C. Chong, "Structural and Optical Properties of Co-Doped ZnO Thin Films," *J. Supercond.*, vol. 18, no. 1, pp. 97–103, Feb. 2005, doi: 10.1007/s10948-005-2158-4.

[13] S. J. Pearton *et al.*, "Advances in wide bandgap materials for semiconductor spintronics," *Mater. Sci. Eng. R Reports*, vol. 40, no. 4, pp. 137–168, Feb. 2003, doi: 10.1016/S0927-796X(02)00136-5.

[14] Y. Y. Villanueva, D.-R. Liu, and P. T. Cheng, "Pulsed laser deposition of zinc oxide," *Thin Solid Films*, vol. 501, no. 1–2, pp. 366–369, Apr. 2006, doi: 10.1016/j.tsf.2005.07.152.

[15] M. Opel, S. Geprägs, M. Althammer, T. Brenninger, and R. Gross, "Laser molecular beam epitaxy of ZnO thin films and heterostructures," *J. Phys. D. Appl. Phys.*, vol. 47, no. 3, p. 034002, Jan. 2014, doi: 10.1088/0022-3727/47/3/034002.

[16] P. B. Taunk, R. Das, D. P. Bisen, R. K. Tamrakar, and N. Rathor, "Synthesis and optical properties of chemical bath deposited ZnO thin film," *Karbala Int. J. Mod. Sci.*, vol. 1, no. 3, pp. 159–165, Nov. 2015, doi: 10.1016/j.kijoms.2015.11.002.

[17] G. Shanmuganathan and I. B. S. Banu, "Influence of Codoping on the Optical Properties of ZnO Thin Films Synthesized on Glass Substrate by Chemical Bath Deposition Method," *Adv. Condens. Matter Phys.*, vol. 2014, pp. 1–9, 2014, doi: 10.1155/2014/761960.

[18] F. U. Hamelmann, "Thin film zinc oxide deposited by CVD and PVD," *J. Phys. Conf. Ser.*, vol. 764, p. 012001, Oct. 2016, doi: 10.1088/1742-6596/764/1/012001.

[19] O. Fouad, A. Ismail, Z. zaki, R. Mohamed, "Zinc oxide thin films prepared by thermal evaporation deposition and its photocatalytic activity," *Appl. Catal. B Environ.*, vol. 62, no. 1–2, pp. 144–149, Jan. 2006, doi: 10.1016/j.apcatb.2005.07.006.

[20] K. Lefatshe, C. M. Muiva, and L. P. Kebaabetswe, "Extraction of nanocellulose and in-situ casting of ZnO/cellulose nanocomposite with enhanced photocatalytic and antibacterial activity," *Carbohydr. Polym.*, vol. 164, pp. 301–308, May 2017, doi: 10.1016/j.carbpol.2017.02.020.

[21] M. Ohmukai, T. Nakagawa, and A. Matsumoto, "ZnO Films Deposited on Glass by Means of DC Sputtering," *J. Mater. Sci. Chem. Eng.*, vol. 04, no. 10, pp. 1–7, 2016, doi: 10.4236/msce.2016.410001.

[22] S. M. Pawar, B. S. Pawar, J. H. Kim, O.-S. Joo, and C. D. Lokhande, "Recent status of chemical bath deposited metal chalcogenide and metal oxide thin films," *Curr. Appl. Phys.*, vol. 11, no. 2, pp. 117–161, Mar. 2011, doi: 10.1016/j.cap.2010.07.007.

[23] T. Srinivasulu, K. Saritha, and K. T. R. Reddy, "Physical Properties of Spray Deposited Fe:ZnOThin Films," *Mater. Today Proc.*, vol. 4, no. 14, pp. 12571–12576, 2017, doi: 10.1016/j.matpr.2017.10.063.

[24] T. Minami, H. Sato, H. Nanto, and S. Takata, "Group III Impurity Doped Zinc Oxide Thin Films Prepared by RF Magnetron Sputtering," *Jpn. J. Appl. Phys.*, vol. 24, no. 10A, p. L781, Oct. 1985, doi: 10.1143/JJAP.24.L781.

[25] J. C. Kim and E. Goo, "Morphology and formation mechanism of the pyrochlore phase in ZnO varistor materials," *J. Mater. Sci.*, vol. 24, no. 1, pp. 76–82, Jan. 1989, doi: 10.1007/BF00660935.

[26] S. Bethke, H. Pan, and B. W. Wessels, "Luminescence of heteroepitaxial zinc oxide," *Appl. Phys. Lett.*, vol. 52, no. 2, pp. 138–140, Jan. 1988, doi: 10.1063/1.99030.

[27] G. Demircan *et al.*, "The effect of Co and Mn Co-Doping on structural and optical properties of ZnO thin films," *Opt. Mater. (Amst).*, vol. 126, p. 112163, Apr. 2022, doi: 10.1016/j.optmat.2022.112163.

[28] C. M. Firdaus, M. S. B. S. Rizam, M. Rusop, and S. R. Hidayah, "Characterization of ZnO and ZnO: TiO2 Thin Films Prepared by Sol-Gel Spray-Spin Coating Technique," *Procedia Eng.*, vol. 41, pp. 1367–1373, 2012, doi: 10.1016/j.proeng.2012.07.323.

[29] B. P. Kafle, S. Acharya, S. Thapa, and S. Poudel, "Structural and optical properties of Fe-doped ZnO transparent thin films," *Ceram. Int.*, vol. 42, no. 1, pp. 1133–1139, Jan. 2016, doi: 10.1016/j.ceramint.2015.09.042.

[30] R. Saleh, S. P. Prakoso, and A. Fishli, "The influence of Fe doping on the structural, magnetic and optical properties of nanocrystalline ZnO particles," *J. Magn. Magn. Mater.*, vol. 324, no. 5, pp.

665–670, Mar. 2012, doi: 10.1016/J.JMMM.2011.07.059.

[31] J. Shi, J. Zhang, L. Yang, M. Qu, D. Qi, and K. H. L. Zhang, "Wide Bandgap Oxide Semiconductors: from Materials Physics to Optoelectronic Devices," *Adv. Mater.*, vol. 33, no. 50, Dec. 2021, doi: 10.1002/adma.202006230.

[32] D. Akcan, "Determination of optical constants and band gap variation of Zn0.98-xCu0.02MgxO thin films," *Front. Life Sci. Relat. Technol.*, vol. 3, no. 3, pp. 101–106, Dec. 2022, doi: 10.51753/flsrt.1120679.

[33] E. Burstein, "Anomalous Optical Absorption Limit in InSb," *Phys. Rev.*, vol. 93, no. 3, pp. 632–633, Feb. 1954, doi: 10.1103/PhysRev.93.632.

[34] L. S. Wang *et al.*, "Preparation and characterization of the ZnO:Al/Fe65Co35/ZnO:Al multifunctional films," *Appl. Phys. A*, vol. 106, no. 3, pp. 717–723, Mar. 2012, doi: 10.1007/s00339-011-6679-3.